A Study on mm-Wave Propagation in and Around Buildings

LEONARDO POSSENTI[1], MARINA BARBIROLI [1], ENRICO M. VITUCCI [1] (Senior Member, IEEE), FRANCO FUSCHINI [1], MATTIA FOSCI[2], AND VITTORIO DEGLI-ESPOSTI [1] (Senior Member, IEEE)

[1]Department of Electrical, Electronic and Information Engineering "G. Marconi," University of Bologna, 40126 Bologna, Italy

[2]Design Engineering Team, JMA Italia/TEKO TELECOM s.r.l., 40024 Bologna, Italy

CORRESPONDING AUTHOR: M. BARBIROLI (e-mail: marina.barbiroli@unibo.it)

ABSTRACT mm-waves are envisaged as a key enabler for 5G and 6G wireless communications, thanks to the wide bandwidth and to the possibility of implementing large-scale antenna arrays and advanced transmission techniques, such as massive MIMO and beamforming, that can take advantage of the multidimensional properties of the wireless channel. In order to analyze in depth the peculiar characteristics of mm-wave propagation, joint measurement and simulation campaigns in indoor and outdoor microcellular environments have been carried out. The investigation highlights that the assumption that mm-wave NLoS connectivity is hardly feasible is not necessarily true as significant reflections, scattering and even transmission mechanisms can provide good NLoS coverage in the considered indoor and outdoor scenarios. This is also reflected in the limited angle-spread differences between LoS and NLoS locations in some cases. Finally, the contribution of different propagation mechanisms (reflection, diffraction, scattering and combination of them) to the received signal is analyzed in the paper with the help of ray tracing simulations. These outcomes can be helpful to predict the performance of mm-wave wireless systems and for the development of deterministic and geometric-stochastic mm-wave channel models.

INDEX TERMS Channel modeling, mm-waves, propagation mechanisms, ray-tracing.

I. INTRODUCTION

IN ORDER to cope with the explosive growth of data rate demand and given the sub-6 GHz spectrum shortage, millimeter wave (mm-wave) frequencies (~30-300 GHz) have been considered for 5G systems and beyond [1], [2], [3], [4], [5]. The primary motivation for using the mm-wave spectrum is its high data-rate and low latency potential due to the large available bandwidth, which can enable services with very stringent requirements, such as wireless cognition, centimeter-level location and ultra-reliable, low-latency communications for industrial or vehicular environment. Moreover, higher frequencies allow for the use of smaller antenna elements, and therefore of massive antenna arrays and advanced transmission techniques, e.g., massive MIMO and pencil-beamforming which are envisioned to be key enablers for future systems [1]. Furthermore, massive arrays, due the high-gain beams, can compensate for the very high isotropic attenuation at these frequencies, and also provide increased capacity in high-density, multiple users scenarios [6].

The effectiveness of multiantenna techniques rely on the multidimensional and spatial properties of the wireless channel, as these technologies necessitate special strategies [7] for beam acquisition and tracking. Therefore, the design, deployment and simulation of mm-wave wireless systems will surely benefit from a thorough multipath propagation characterization.

Extensive measurement campaign analysis [8], [9], [10], [11] have shown that high-frequency communications face limitations in terms of power budget, compared to the sub-6 GHz band. Diffractions around, and transmissions through obstacles are weaker at mm-wave frequencies, while

significant paths, apart from the line-of-sight (LoS) one when present, are often limited in number and spatially sparse. Some studies have tried to analyze in depth mm-wave propagation, i.e., what propagation processes actually generate such channel characteristics [12], [13], [14], but some important issues related to the actual reverberation degree of mm-wave indoor propagation, the relative importance of multiple-bounce vs. single-bounce reflections, of diffraction vs. diffuse scattering have not been completely addressed so far.

Such issues are important to develop and to properly parametrize fast and reliable ray-based, spatially consistent, deterministic or geometric-stochastic, propagation models, needed for the design, deployment and functioning of the coming wireless systems. In particular, recent research advocates for the real-time use of deterministic ray-based propagation models to help initial beam acquisition and tracking or as a proxy of measurements to train Machine Learning based channel models [15], [16].

Therefore, beyond the validation of the Ray Tracing (RT) simulation tool at mm-waves, this paper aims at filling the gaps in the comprehension/identification of the relevant propagation mechanisms at mm-waves. Directional measurements and RT simulations of indoor and outdoor short-range propagation environments at 27 GHz and 38 GHz are combined to investigate channel properties, such as angular dispersion in LoS and NLoS conditions, multipath richness in indoor environment, the relative importance of multiple-bounce vs. single-bounce reflections, of diffraction vs. diffuse scattering and the relevance of through-wall transmission, taking into account the different environment characteristics.

The considered scenarios are typical indoor and outdoor environments in the proximity of buildings, where a high density of users, with different requirements in terms of QoS, is expected. All the environments show large spaces with a significant number of scattered elements (columns, stairs, doors, plants, walls of different materials) and therefore are quite suitable for the characterization of mm-wave multipath propagation.

The paper is organized as follows: in Section II measurements are firstly described with the measurements set-up, then in Section III the RT simulations are presented, while in Section IV results of the measurement campaigns and the simulation outputs are shown, finally Section V includes the main conclusions of this work.

II. MEASUREMENT CAMPAIGNS
Directional measurements at 27 and 38 GHz have been first performed in a large-indoor environment in the hall of the School of Engineering of the University of Bologna, then in an outdoor setting in the courtyard of the same School, using a portable spectrum analyzer and a rotating positioner with directive antennas over multiple receiving points. Since the measurement set-up includes only one rotating positioner, the TX and the RX are set at the same height in order to analyze the azimuth-angle characteristics of the channel. The

TABLE 1. Summary of the measurement set-up.

	Environment type	Sounding method @ the RX	# of LoS locations	# of NLoS locations
UniBO Indoor	Large indoor (mall, railway hall, airport hall)	Directional in azimuth	4	7
UniBO Outdoor	Dense urban outdoor, restricted open area	Directional in azimuth	2	5
JMA Indoor Office	Office indoor (open space with plasterboard partitions)	Fixed in azimuth and elevation	14	12
JMA Indoor Corridor	Office indoor	Fixed in azimuth and elevation	3	37

rotating positioner was used at the RX side, while the TX antenna was fixed, which can mimic a realistic use case and ensures a sufficient link power-budget. It is worth noting that this single-directional setup will probably reduce the number of paths with respect to what can be measured with a fully double directional setup and a powerful amplifier. But it's also true that the focus of the study is the determination of the relevant propagation mechanisms, and there is no reason to think that a directional setup will favor one propagation mechanism -other than the LoS - over others.

In order to increase environment diversity, further measurements (non-directional) have been carried out at the frequency of 28 GHz in a typical open-plan indoor office environment located in the main headquarter of the company TEKO-JMA Wireless, Castel S. Pietro, Italy.

For convenience, the measurement setup is summarized in Table 1.

As shown in Table 1, the four measurement environments have been selected as representative of typical environments where the mm-wave transmission use is foreseen, namely large indoor, dense urban outdoor, and indoor office.

A. UNIVERSITY MEASUREMENT SETUP
The equipment used to sound the radio channel is a portable Spectrum Compact Analyzer (SCA) by SAF Tehnika [17], composed of a spectrum analyzer, a continuous wave signal generator and two horn antennas, along with cables, connectors and two tripods. The SCA is a very light, battery-powered analyzer, which is an attractive solution because of its portability and easy use.

The signal analyzer is connected through an USB cable to the laptop to store the information of the received signal using a dedicated proprietary software GUI. The signal generator is instead connected to the transmitting antenna. The directive horn antennas operate in a frequency band ranging from 26.5 GHz to 40.5 GHz and the considered frequencies are the 27 GHz and the 38 GHz, as they are two frequencies of interest for 5G. Technical data are reported in Table 1.

TABLE 2. University measurements set-up.

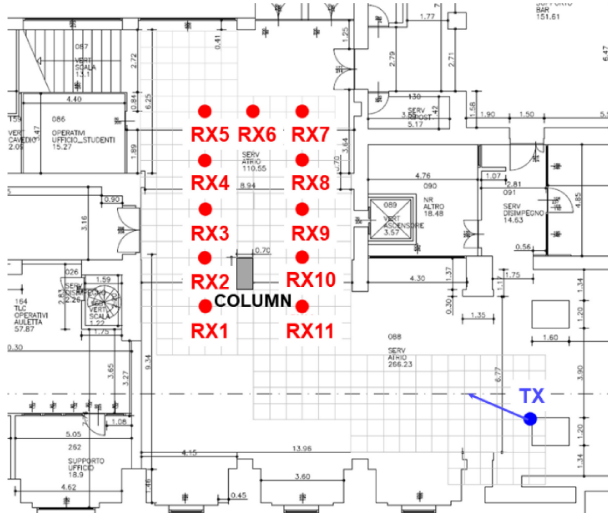| Frequency	Antenna gain [dBi]	Antenna HPBW	TX Output Power [dBm]
27 GHz	20.5	E-plane: 14° H-plane: 17.5°	5
38 GHz	21.5	E-plane: 11.5° H-plane: 13°	5

FIGURE 1. Map of the entrance hall of the School of Engineering of Bologna University.

Through a rotating antenna positioner, the receiver is steered to scan the channel from each angular direction, in the azimuth plane (0°-360°), with a step of 15°, for a total of 24 directions.

B. UNIVERSITY MEASUREMENT CAMPAIGN

Indoor channel measurements are conducted in the entrance hall of the School of Engineering of the University of Bologna (UniBO), reported in Fig. 1. The environment is an open space, almost empty, with sparse corners and a central column, made of travertine. The floor is entirely made of a particular type of marble, while the walls are composed by travertine. In the top side of the figure, there is a large, windowed glass wall. Ceiling is at a height of 5-6 meters.

The measurement arrangement is sketched in Fig. 1, the TX unit is located at the bottom-right corner of the figure (blue dot), whereas the RX unit is placed in 11 different central locations in the room (red dots), both in LoS (RX1, RX3, RX10, RX11) and in NLoS locations. The height of TX and RX antennas are the same for all positions (2.1 m). The TX is pointing towards the direction of the RXs (blue arrow in Fig. 1), so as for the RXs to fall inside the main lobe of the TX antenna. The environment is kept almost static during the measurement.

Outdoor channel measurements are carried out in the internal yard, around buildings of the School of Engineering of the University of Bologna, reported in Fig. 2. The environment has an open garden surrounded by high buildings
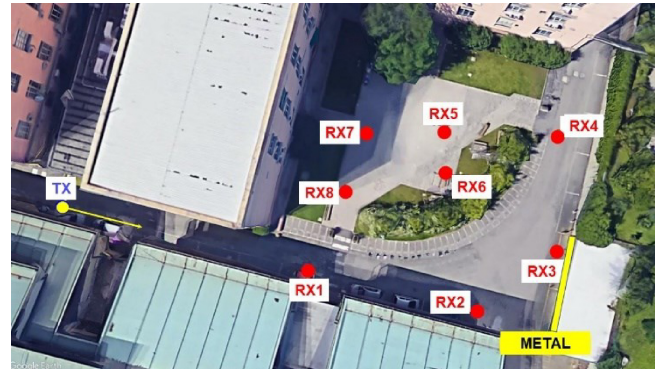

FIGURE 2. Outdoor courtyard in the School of engineering of Bologna University.

and a short canyon-street, where the transmitter is placed. The TX is pointing along the small street canyon as shown in Fig. 2 (yellow arrow).

The construction at the bottom-right corner is made of metal (yellow line in Fig. 2). The RX unit is placed in 8 different locations both in LoS (RX1 and RX2) and in NLoS. TX and RX antennas were kept at the same height for all positions (2.1 m).

C. JMA MEASUREMENT SETUP

Measurements in the indoor office environment have been carried out using a 5G New Radio (NR) transceiver, which generates an OFDM signal at the frequency of 27.925 GHz, with a bandwidth of 100 MHz. The average power on the bandwidth was considered, by sounding the so-called Reference Signal Received Power (RSRP).

In particular, the received power has been recorded with a portable Real-Time Spectrum Analyzer (VIAVI Celladvisor 5G), which was able to demodulate the NR signal and to extract the RSRP.

The TX antenna is a 16-elements planar array with 12 dBi maximum gain, half-power beamwidth of 60° in the horizontal plane and circular polarization, which was kept with a fixed orientation (Fig. 3), while the receiving antenna is an omnidirectional vertically polarized antenna, with 3 dBi maximum gain. The measurement set-up allows for all the receiver locations in the "Meeting Room" to be within the main lobe of the TX antenna (strong LoS condition), while the receivers in the "Guest Room" are outside the main lobe of the TX antenna and in NLoS condition, then allowing to better analyse the effect of multipath on the received power. For this scenario, only narrowband results are presented in the following due to the different receiving equipment.

D. JMA MEASUREMENT CAMPAIGN

The measurement scenario at the JMA Wireless company is an office environment, which consists of an open space with a meeting room and a small guest room located in its center and separated each other and from the outside through partition walls made by plasterboard (see Fig. 3 (a)). The TX equipment is located at the bottom of the meeting room, and the TX array is pointed perpendicularly
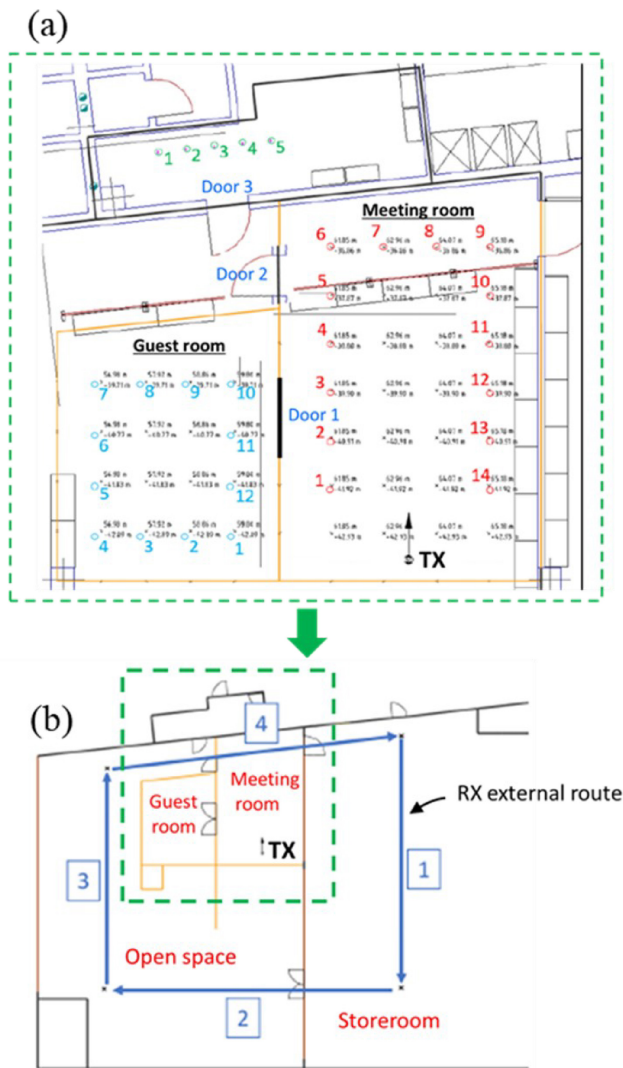
FIGURE 3. Map of the office measurement scenario at JMA Wireless, with TX location, internal (a) and external (b) RX locations.

TABLE 3. UniBO RT simulation settings.

Maximum number of interactions for each ray	7
Maximum number of reflections for each ray	5
Maximum number of diffractions for each ray	2
Maximum number of transmissions for each ray	2
Maximum number of scatterings for each ray	1
Combined reflections and diffractions	Yes (max 3)
Combined scattering and reflections	Yes (max 1)

A. UNIBO RT TOOL

The RT model developed in house at the University of Bologna, also called 3DScat in the following, is an image-based 3D RT tool [18], [19], capable of simulating multipath propagation in indoor and outdoor environments with multiple interactions, including specular reflection, transmission, diffraction, diffuse scattering and any combination of these. In particular, diffuse scattering is simulated here using the Effective Roughness (ER) heuristic model in order to take into account non-specular scattering due to environment details (surface roughness, decorations, furniture, smaller objects) that are not described in the environment database. A directive scattering pattern and standard values of the scattering parameter S between 0.3 and 0.5, have been used for smooth and for irregular surfaces, respectively.

The objective of RT simulations is two-fold. The first one is to calibrate and validate the tool against the mm-wave measurements. To support reliable channel predictions the electromagnetic parameters (i.e., the complex relative permittivity) of the different walls and environment objects for the two frequencies have been derived from literature surveys [20], [21] (e.g., values for the plasterboard of the JMA Wireless scenario, Fig. 3) and through the Fabry-Pérot (FP) method presented in [22] (e.g., values for the marble floor in the University Hall, scenario in Fig. 1). The FP method is useful for the item-level investigation on the e.m. properties of construction materials in the form of slabs.

The second significant objective is to use RT to investigate and interpret the measurement results by analyzing the propagation mechanisms (e.g., number and types of bounces) corresponding to each contribution that shows-up as a measured, angle-related contribution. The analysis of the multidimensional propagation mechanisms and the identification of the dominant ones as a function of the environment and the considered frequency is fundamental to correctly plan mm-waves networks.

An additional goal, that will be pursued in the follow-on of the present work, is to evaluate RT as a real-time channel prediction tool to assist beamforming techniques (RT-assisted beamforming [15]).

The fundamental structures of the room, such as main walls, floor and ceiling, metal rods and windows, are considered in RT simulations. The main RT-simulation interaction parameters are summarized in Table 3: the choice of the maximum number of enabled interactions is a trade-off between computational effort and prediction accuracy.

in the direction of the opposite wall, as indicated by the black arrow in Fig. 3 (a). The receiving equipment has been moved in different locations inside the meeting room (red points, 14 locations), the guest room (blue points, 12 locations), and the corridor in front of them (green points, 5 locations). Moreover, additional measurements have been done along an "external" receiving route as shown in Fig. 3 (b), where the receiver has been moved all around the 2 rooms, in the external open space and in the adjacent storeroom located on the right side of the map.

III. RT SIMULATIONS

In order to interpret measurement results, validate the RT model and analyse the main propagation mechanisms taking place in the different environments, measurements have been complemented with RT simulations using two different tools as clarified in the following Sections III-A and III-B.

TABLE 4. RMSE between measurement and simulations in indoor and outdoor environment.

Environment/Frequency (RT tool)	RMSE (simulated received power – measured received power) [dB]
Indoor UniBO hall @ 27 GHz (UniBO RT)	1.37
Indoor UniBO hall @38 GHz (UniBO RT)	1.54
Indoor JMA @ 28 GHz (UniBO RT)	5.2
Indoor JMA @ 28 GHz (iBwave)	6.1
Outdoor UniBO @ 27 GHz (UniBO RT)	4.7
Outdoor UniBO @38 GHz (UniBO RT)	3.6

FIGURE 4. Measured and simulated PL, and 3GPP InH model, as a function of the distance, for the indoor UniBO environment @ 38 GHz.

B. IBWAVE RT TOOL

For the indoor office scenario at TEKO-JMA, the 3DScat RT simulations are also compared with additional simulations performed using the iBwave tool [23], a commercial suite currently used by the TEKO-JMA company, acknowledged as a reference tool for the planning of wireless networks. iBwave includes a "simplified" RT engine which is able to simulate, in addition to the direct (LoS) path, transmission through walls and single-bounce specular reflection.

IV. RESULTS

In this section, the indoor and outdoor measurements and simulations at the two considered frequencies are analyzed and compared to investigate the channel propagation characteristics and to evaluate RT performances.

A. NARROWBAND ANALYSIS

As a first step, the received power and the Path Loss (PL) extracted from measurements in the different scenarios are compared with RT simulations. Regarding the directional measurements carried out in the University scenarios, measured and RT-simulated received power values are compared for all the 24 RX antenna azimuth orientations. In Table 4 simulation performance in terms of RMSE is reported for all the scenarios considered in this study.

The good performance of the RT model is evident, especially in the simple, empty and large environment of the entrance hall of the Engineering School. In Fig. 4, the 38 GHz local-average PL for each RX location of the indoor hall scenario is reported as a function of the distance, for both measurements (square markers) and RT simulations (star markers). LoS and NLoS receivers are represented in the figure with different colours, blue and black, respectively.

Measured/simulated PL is also compared with the reference propagation models proposed by ITU-T and 3GPP for IMT-2020 system simulations [24]. Specifically, PL values have been compared with the Indoor Hotspot model (InH) described in [24], for both the LoS (blue dashed line) and NLoS (black dashed line) cases. The InH scenario is intended to take into account various typical indoor deployment cases including offices, open areas, corridors and shopping malls
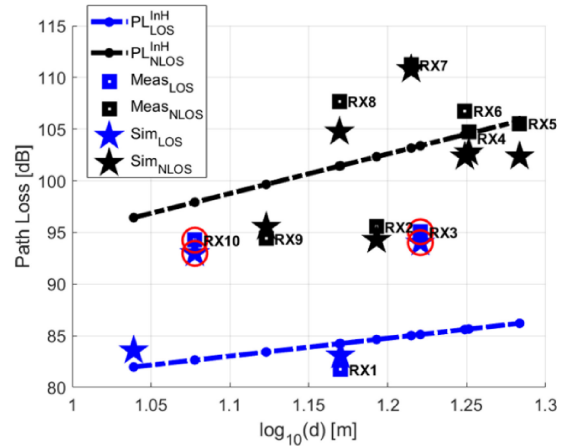
with transmitters at a height of 2-3 m and receivers are at a height of 1.5 m.

As can be noted from Fig. 4 there are some RX locations in a quasi-LoS condition (RX3 and RX10), meaning that they are directly visible from the TX but the Fresnel ellipsoid is partly obstructed. Such receivers (highlighted by the red circle marker) have a very different measured PL compared to what predicted by 3GPP model, being their PL close to the one of NLoS locations. This behaviour is probably due to the low contribution of diffraction and to the critical, sharp transition on the visibility boundary (as reported in Section IV-C) at mm-waves.

A similar trend has been found at 27 GHz, highlighting that a deterministic approach based on an accurate description of the environment is more suitable at mm-wave frequencies, where the traditional LoS/NLoS classification can lead to large errors.

In Fig. 5 similar results are shown for the indoor office (JMA Wireless, Fig. 3) environment at 28 GHz.

In the plots, measurements are represented with blue triangles, while RT simulations have been carried out using both the UniBO RT tool (orange diamonds) and the commercial iBwave tool (red squares), moreover the red dotted line reports the simulation values for the 3GPP InH model. Results are shown separately for the LoS/quasi-LoS locations (Fig. 5 (a)) and NLoS locations (Fig. 5 (b)), as described in the map in Fig. 3. In both cases, the average path loss values (both measured and simulated) have a trend which is in good agreement with the 3GPP InH reference model. It is worth noting that both RT tools show a good agreement with measurements. From simulations some insight about propagation mechanisms can be inferred: in the JMA office environment propagation is dominated by the LoS path (for the "Meeting Room") or low-loss NLoS paths transmitted through the light partition walls (for the "Guest Room"). In other terms, in most NLoS locations of the considered office environment transmission through walls is the dominant propagation mechanism, as it will be shown in the following (see Section IV-C), due to the small
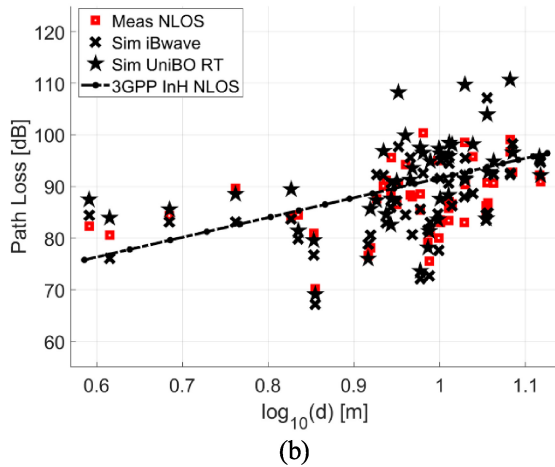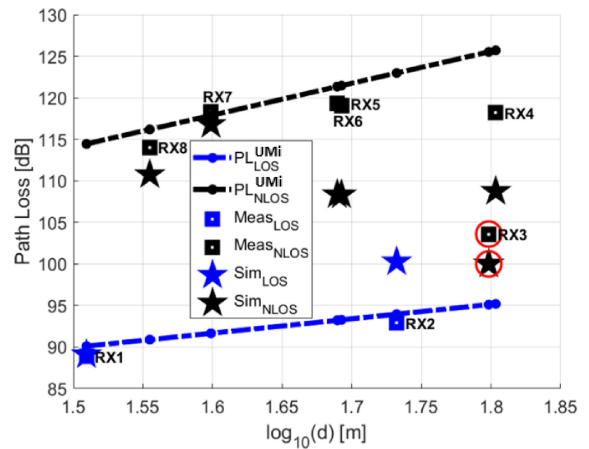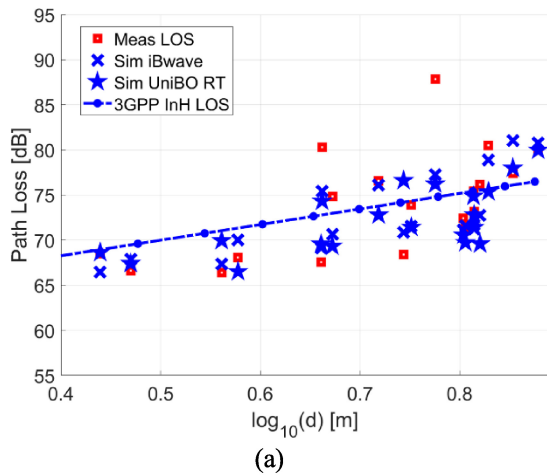
(a)

(b)

FIGURE 5. Measured PL and simulated PL (using both the iBwave and the 3DScat tools) and 3GPP InH model as a function of the distance for the indoor JMA environment @ 28 GHz: (a) LoS or quasi-LoS cases; (b) NLoS cases.
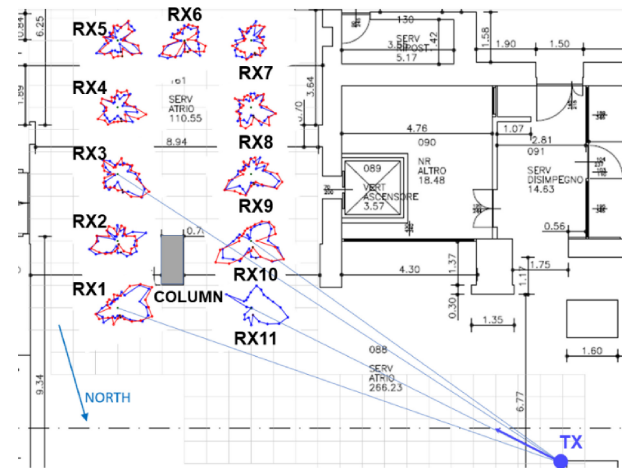

FIGURE 6. Measured and simulated PL, and 3GPP UMi model, as a function of the distance, for the outdoor UniBO environment @ 38 GHz.

FIGURE 7. Measured PAPs for the indoor UniBO scenario @ 27 GHz (blue line) and 38 GHz (red line).

attenuation of plasterboard partition walls. Therefore, this kind of open-plan indoor environments are quite suitable for 27 and 38 GHz transmission despite the presence of partition walls, as confirmed by the high levels of received power generally observed.

In Fig. 6 outdoor measurements at the University campus are compared with the Urban Micro (UMi) model.

The Umi scenario is intended to represent street canyons and open areas, with the transmitter mounted below the rooftop levels of surrounding buildings (less than 10 m), and the receivers are at a height of 1.5-2.5 m.

Furthermore, also in this outdoor scenario there are some RXs in a quasi-LoS condition, e.g., RX3 (highlighted by the red circle marker), where the 3GPP model doesn't perform well. The lower value of the PL with respect to the NLoS case, may be due to the presence of strong reflections on the metal advertising board panel located behind the RX3.

B. ANGULAR DOMAIN ANALYSIS

In order to investigate the multipath spatial properties of the wireless channel, a directional survey is considered in both indoor and outdoor University scenarios (see Fig. 1

and Fig. 2). Both the Power Angle Profile (PAP) related to the (azimuth) angle-of-arrival at the RX side and the Angle Spread (AS) have been considered. Since the PAPs depend on the environment and on each RX location, they have been plotted over the environment layout at each RX position, as shown in Fig. 7 and Fig. 8 for the indoor and outdoor case, respectively. PAPs at 27 and 38 GHz are depicted using blue and red colors, respectively.

In Fig. 7 the LoS path is highlighted with blue lines, where present.

In Fig. 9 the simulated (blue) and measured (red) PAP plots are shown for receivers RX11 an RX2 at 27 GHz in indoor scenario. The RMSE value is of 4.6 dB and 5.1 dB for receiver RX11 (LoS) and receiver RX2 (NLoS) respectively, which confirms the accuracy of the RT tool. From Fig. 9 it is evident that the AS is larger in NLoS condition (Fig. 9 (b)), than in LoS condition (Fig. 9 (a)), as it should be due to the presence of the dominant LoS path in the latter case.

This result is confirmed in Fig. 10, where the AS values are quite correlated to the LoS/NLoS condition. Conversely,
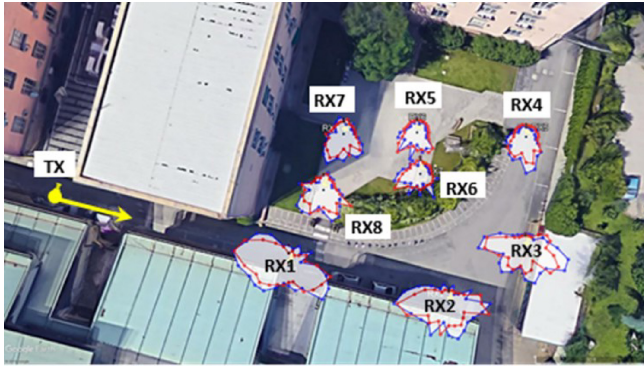
FIGURE 8. Measured PAPs for the outdoor UniBO scenario @ 27 GHz (blue line) and 38 GHz (red line).
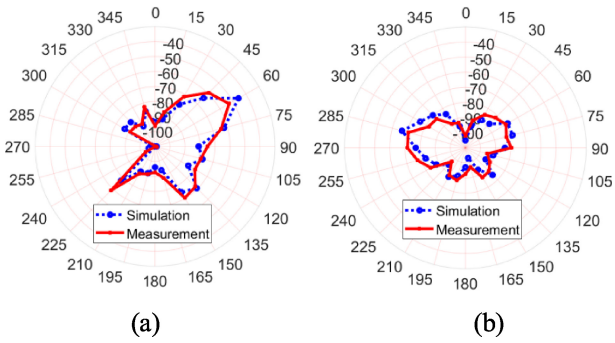

FIGURE 9. Comparison between measured and simulated PAP for the indoor UniBO scenario @ 27 GHz: (a) RX11 (LoS); (b) RX2 (NLoS).
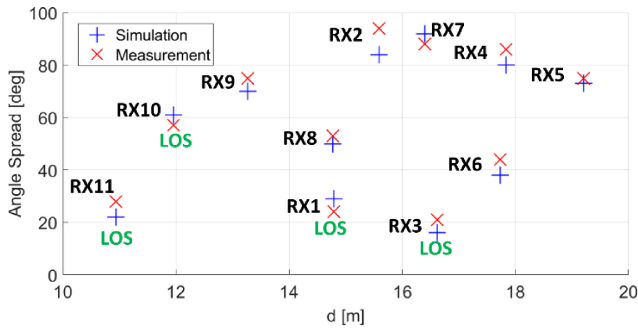

FIGURE 10. Comparison between measured and simulated AS for the indoor UniBO scenario @ 27 GHz as a function of the TX-RX distance.

FIGURE 11. Comparison between measured and simulated AS for the outdoor UniBO scenario @ 27 GHz as a function of the TX-RX distance.

FIGURE 12. Cumulative probability distribution function of AS in the indoor UniBO scenario @ 27 GHz (a) and 38 GHz (b).

they seem rather independent from the distance between TX and RXs.

RX10, which is in LoS, has a high AS, probably because in addition to the strong lobe in the LoS direction, there are also other two strong lobes coming from strong reflections from the central column and from the wall as reported in Fig. 7.

With reference to the outdoor case, results reported in Fig. 11, confirm that angular dispersion is basically not affected by link distance. Differently from indoor, the AS looks weakly correlated also to the LoS/NLoS condition. As a matter of fact, the NLoS receiver RX4 shows a quite low AS, probably due to some strong signal contributions coming from the metal wall highlighted in Fig. 2 and Fig. 8. At
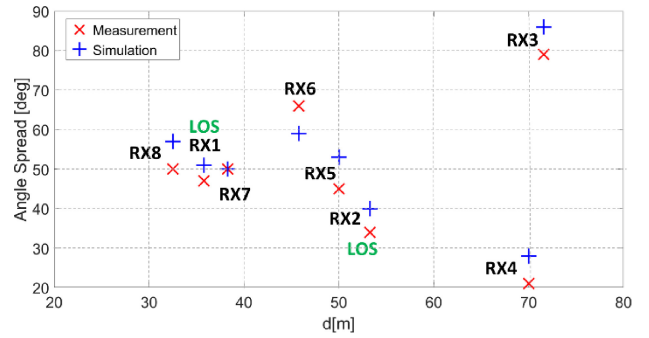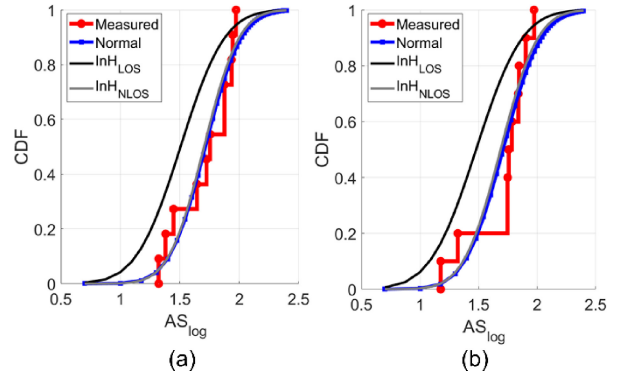
the same time, strong reflections are also likely to be present at RX1, thus increasing the AS in spite of the LoS condition. Although the lack of correlation between LoS/NLoS condition and AS is influenced by the characteristics of the investigated scenario, the result has general validity for the case of dense urban scenarios, since strong reflectors such as advertising panels or glass walls with metal-film are very common in urban environment.

In conclusion, strong multipath components seem to rise up in some indoor and outdoor locations, thus greatly affecting signal propagation in both LoS and NLoS conditions, increasing the angle spread in the former case but instead reducing angular dispersion in the latter.

Fig. 12 and Fig. 13 show the cumulative distribution functions (CDFs) plotted as a function of logarithmic AS, defined as [24]: $AS_{log} = \log10(AS/1°)$, for the two considered frequencies in indoor and outdoor scenario respectively. The AS for indoor scenario are in the range of $21° - 94°$ for 27 GHz and $15° - 93°$ for 38 GHz, while the outdoor ASs are in the range of $21° - 79°$ for 27 GHz and $32° - 73°$ for 38 GHz.

All the measured AS values (in red) are fitted with a Gaussian distribution $N \sim (\mu, \sigma^2)$, according to the Least Squares Method, and plotted in Fig. 12 and Fig. 13 with a blue line. The distribution parameters μ and σ – i.e., mean value and standard deviation – are shown in Table 5 and Table 6 for the indoor and outdoor scenario, respectively.
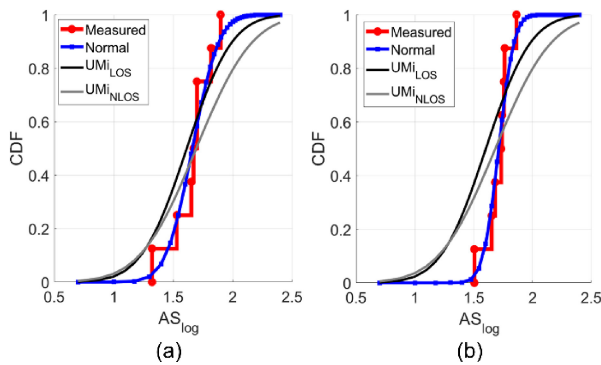
FIGURE 13. Cumulative probability distribution function of AS around buildings (outdoor UniBO scenario) @ 27 GHz (a) and 38 GHz (b).

TABLE 5. Gaussian distribution parameters of measured AS vs 3GPP AS model (indoor scenario).

		3GPP MODEL		MEASUREMENT	
		μ	σ	μ	σ
27 GHz	LoS	1.5060	0.2927	1.7159	0.2374
	NLoS	1.7038	0.2327		
38 GHz	LoS	1.4787	0.3099	1.7096	0.2555
	NLoS	1.6880	0.2499		

TABLE 6. Gaussian distribution parameters of measured AS vs 3GPP AS model (outdoor scenario).

		3GPP MODEL		MEASUREMENT	
		μ	σ	μ	σ
27 GHz	LoS	1.6142	0.3003	1.6618	0.1756
	NLoS	1.6942	1.6827		
38 GHz	LoS	1.6027	0.3023	1.7119	0.1041
	NLoS	1.6827	0.3796		

In general, measurements at 38 GHz and/or outdoor locations tend to have smaller AS with respect to 27 GHz and/or indoor locations, highlighting a higher degree of multipath richness in outdoor environment and for lower frequencies.

In Figs. 12–13 a comparison between the cumulative distribution functions of the measured AS values and the AS values obtained with the 3GPP InH and Umi models for indoor and micro outdoor scenarios is shown. Moreover, Table 5 reports the gaussian distribution parameters (μ and σ) for the 3GPP models and for measurements in indoor scenario. It is clear that the NLoS case is in good agreement with the measured indoor data.

In Table 6 the gaussian distribution parameters are extracted for the outdoor scenario. The LoS case shows a better agreement with the measured data (see Table 6), even though in the outdoor measurements there is a combination of LoS, quasi-LoS and NLoS RXs.

C. ANALYSIS OF PROPAGATION MECHANISMS

Once validated in the considered environments, the RT tool has been used for evaluating the contribution of the different propagation mechanisms – namely reflection, diffraction,
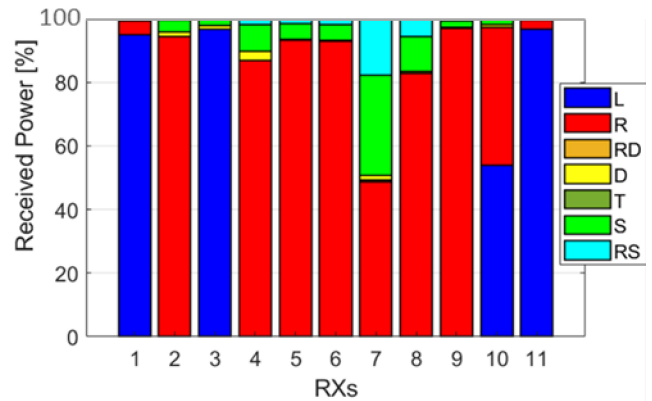

FIGURE 14. Indoor scenario - Contribution of the different propagation mechanisms to the total received power @ 27 GHz.
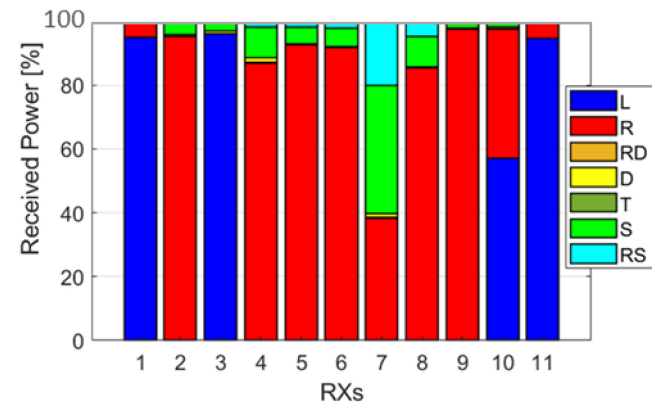

FIGURE 15. Large indoor scenario - Contribution of the different propagation mechanisms to the total received power @ 38 GHz.

diffuse scattering and combinations of them, as summarized in Table 3 – to the total received power.

In Fig. 14 and Fig. 15 the simulation results for the large indoor scenario at 27 GHz and 38 GHz, respectively, are reported.

For LoS receivers (RX1, RX3, RX11 and RX10) and for both frequencies almost 100% of the total received power is due to the direct ray (L), except for RX10, where a strong contribution from reflection (43%) is observed, probably a single-bounce reflection coming from the central column (see Fig. 1 and Fig. 7). Diffraction (D) is almost always negligible, as expected for mm-waves frequencies, as well as combined reflection and diffraction (RD) contributions, which are always below the 3% of the total power.

Reflection is the main propagation mechanism for NLoS receivers. As shown in Fig. 16, also high-order reflections up to the fourth-order are important for strongly NLoS receivers, such as RX7.

Furthermore, the contribution of diffuse scattering is fundamental for strongly NLoS receivers, such as RX7. In this case the 30% and 40% of the total received power @ 27 GHz and 38 GHz respectively is due to scattering, probably because of the presence of a few, big pieces of furniture not taken into account in RT simulation. As reported in
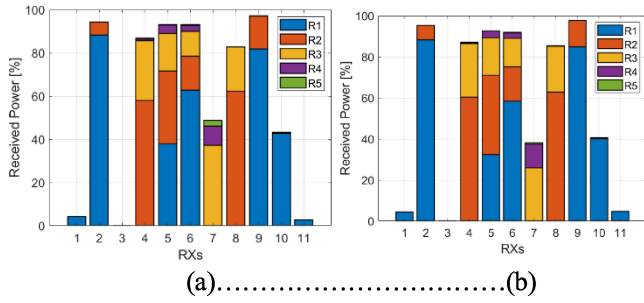
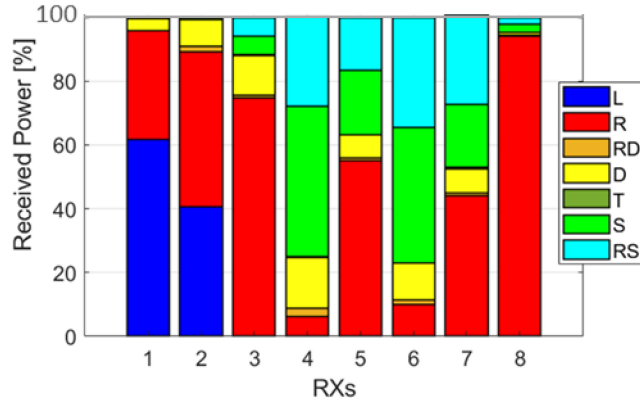FIGURE 16. Insight of the reflection mechanism for 27 GHz (a) and 38 GHz (b) in the large indoor scenario.

FIGURE 18. Outdoor scenario - Contribution of the different propagation mechanisms total received power @ 38 GHz.

FIGURE 17. Outdoor scenario - Contribution of the different propagation mechanisms total received power @ 27 GHz.

FIGURE 19. Insight of Reflection mechanism for 27 GHz (left) and 38 GHz (right) in the outdoor scenario.

Section III, the ER diffuse scattering model implemented in the RT tool accounts for the surface roughness of the walls, decorations or smaller objects not present in the environment database. As shown in Table 3, combined mechanisms have also been considered, such as reflections combined with scattering (RS). The total received power for NLoS receivers, at both frequencies appears to be due to reflections, scattering and a combination of reflections and scattering.

For what concerns the outdoor environment, Fig. 17 and Fig. 18 show simulation results at 27 GHz and 38 GHz respectively.

In the outdoor case the LoS contribution to the total received power is smaller than the indoor scenario, due to the presence of a higher multipath richness: the direct ray component for RX1 and RX2 is 67% and 48% respectively. However, it has to be considered that the TX-RXs distances are higher in this case: 35.8 m and 53.3 m respectively, while in the indoor case the farthest RX is at 16 m.

Specular reflection is significant also in LoS RXs, being greater than 35% for RX1 and almost 50% for RX2 at both frequencies. For NLoS RXs, such as RX3, RX5 and RX8 (see Fig. 17 and Fig. 18), reflection is the main propagation mechanism.

The outcome of this analysis is also confirmed by the specific investigation of the reflection mechanism for the outdoor environment at both frequencies (Fig. 19). Fro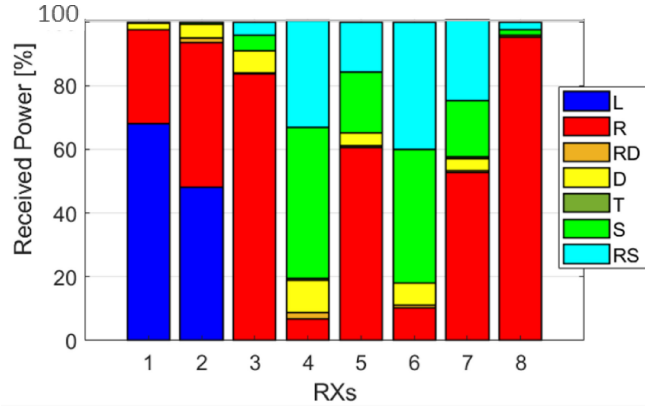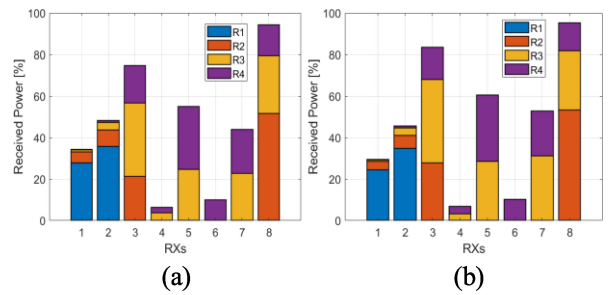m Fig. 19 it can be observed the importance of reflection in NLoS outdoor locations (RX3-RX8), confirmed by the high order of reflections (up to 3 and 4) that contribute to the overall received power, in contrast to the indoor environment (Fig. 16) where relevant reflection contributions are mainly limited to the first or second order.

For NLoS RXs placed in the middle of the yard (RX4 and RX6), scattering alone and reflections combined with scattering are relevant, more than in the indoor case, probably due to the presence of bushes and bicycle stands. Moreover, the diffraction contribution is surprisingly higher in this case. In fact, while in the indoor scenario diffraction is always lower the 3%, for the outdoor case diffraction reaches 10-15%, and even the second-order diffraction is detectable. As an example, Fig. 21 reports the contribution of diffraction in indoor and outdoor scenarios at 27 GHz.

Reflections combined with diffraction and transmissions through walls are in any case negligible.

Finally, in Fig. 21 the analysis of the propagation mechanisms is shown for the indoor office scenario of JMA premises, including both the "internal" and "external" receiver routes (subfigures (a) and (b), respectively).

Interestingly, in most NLoS locations transmission (alone or combined with reflections) is largely dominant with respect to the other mechanisms, due to peculiar characteristics of the environment, which is essentially an open space with plasterboard partition walls.
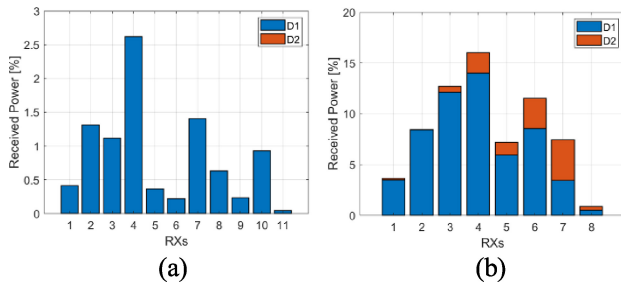
FIGURE 20. Insight of the diffraction mechanism @ 27 GHz for indoor (a) and outdoor (b) scenarios.
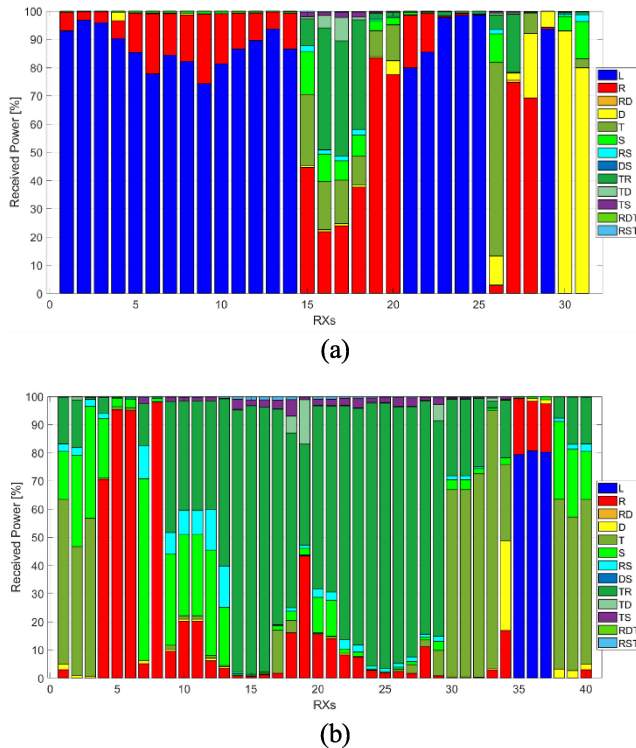

(a)

(b)

FIGURE 21. Contribution of the different propagation mechanisms in the indoor JMA scenario at 28 GHz, for both the internal (a) and external (b) receivers.

Moreover, as already pointed out, reflections of order higher than 2 do not appear to be relevant because of the partition wall characteristics. As in the large indoor environment considered above, scattering, including combination with reflections appears to be significant in all NLoS locations, especially the external ones.

It's also worth noting that in only in a few, very specific cases (e.g., locations 30-31 of Fig. 21 (a)) diffraction can be the dominant mechanism: this usually happens in strongly NLoS locations as in this case, where RX is located on a corridor separated from the adjacent rooms through a thick concrete wall with high penetration loss, and it can be reached only through diffraction on the entrance door opening.

Finally, the number and kind of dominant paths have been extracted from the RT simulations for each RX location, environment and frequency. For the sake of brevity only

TABLE 7. Dominant path contributions for the UniBO outdoor scenario @27 GHz.

RX #		# of rays	% of the overall received power
1	LoS	1	61.6
	Refl	2	21.5
2	LoS	1	40.7
	Refl	2	32.0
3	Refl	7	73.7
	Diff	1	2.3
4	Refl	2	5.2
	Diff	10	12.2
	Scat	20	46.6
	Refl&Scat	8	11.0
5	Refl	7	55.0
	Scat	2	4.5
	Refl&Scat	1	3.1
6	Refl	2	9.5
	Diff	3	4.3
	Scat	15	41.7
	Refl&Scat	6	20.2
7	Refl	3	42.2
	Scat	1	7.1
	Refl&Scat	1	5.7
8	Refl	8	89.0

TABLE 8. Dominant path contributions for the UniBO outdoor scenario @38 GHz.

RX #	Stronger mechanism	# of rays	% of the overall received power
1	LoS	1	68.0
	Refl	2	20.1
2	LoS	1	48.0
	Refl	2	32.0
3	Refl	6	81.1
4	Refl	2	6.0
	Diff	4	4.3
	Scat	18	46.4
	Refl&Scat	10	17.4
5	Refl	7	60.4
	Scat	3	5.8
	Refl&Scat	1	2.7
6	Refl	2	10.0
	Diff	2	2.0
	Scat	13	40.1
	Refl&Scat	7	25.2
7	Refl	3	50.3
	Scat	1	4.5
	Refl&Scat	1	4.3
8	Refl	7	89.0

results for the outdoor UniBo environment @ 27 GHz and 38 GHz are reported in Table 7 and Table 8, respectively.

In the analysis a path is considered to be dominant if its power contribution is within 10 dB with respect to the strongest path.

Interesting information can be extracted from the analysis: reflection is very important as even in LoS conditions (RX1 in Table 7) it accounts for 1/5 of the overall received power.

Surprisingly, diffraction in some locations (RX4 in Table 7) is stronger than reflection alone, while diffuse scattering is confirmed to be one of the dominant propagation mechanisms at mm-waves, also in combination with reflection.

Comparison between Table 7 and Table 8 also highlights a frequency-dependent behaviour: for higher frequencies diffraction is less important than diffuse scattering and the importance of diffuse scattering - alone and combined with reflection - increases as frequency increases, especially in NLoS locations (RX6 in Table 8). It is worth noting that here diffuse scattering means any contribution that cannot be classified as specular reflection from flat surfaces or diffraction from edges, and therefore includes the effect of furniture, vegetation and environment details that are not present in the environment description database.

V. CONCLUSION

The results of measurement and simulation campaigns in mm-wave bands are presented in the paper, aimed at investigating propagation characteristics, and provide insight for the development of mm-wave deterministic and geometric-stochastic propagation models, and for the design and deployment of mm-wave networks.

Results confirm known findings, such as the minor contribution of diffraction with respect to sub-6 GHz frequencies, which leads to large prediction errors in NLoS locations if multiple reflections – up to the fourth order – and diffuse scattering are neglected. Moreover, the analysis of the multipath spatial properties of the wireless channel has shown that the direct path – if present – usually carries most of the power, but strong multipath components can be present, increasing angular dispersion in line of sight and instead reducing it under NLoS conditions with respect to what expected. Furthermore, differences between indoor and outdoor AS values are highlighted as a function of the frequency (38 GHz shows lower AS vs. 27 GHz), and confirming that, due to the presence of possible scatterers commonly present in urban environment, AS is weakly correlated to the LoS/NLoS condition in outdoor cases. Overall, angular dispersion seems basically independent of link distance, but it rather depends on the spatial distribution environment clutter. This finding is further confirmed by the highlighted importance of diffuse scattering due to furniture or minor details, which represents after reflection the most important interaction mechanism.

The indoor analysis has shown that the dominant NLoS propagation mechanism is surprisingly transmission at both frequencies in the office indoor environment, due to the light-material of indoor-partition walls.

Follow-up activities will include the analysis of mm-wave propagation mechanisms in other environments, such as the air-to-ground urban environment, or the extension of the work to sub-THz frequency bands.

REFERENCES

[1] W. Jiang and F.-L. Luo, "Enhanced millimeter-wave wireless communications in 6G," in *6G Key Technologies: A Comprehensive Guide*. Hoboken, NJ, USA: Wiley, 2023, pp. 131–194, doi: 10.1002/9781119847502.ch4.

[2] H. Yi et al., "Ray tracing meets terahertz: Challenges and opportunities," *IEEE Commun. Mag.*, early access, Oct. 31, 2022, doi: 10.1109/MCOM.001.2200454.

[3] D. Serghiou, M. Khalily, T. W. C. Brown, and R. Tafazolli, "Terahertz channel propagation phenomena, measurement techniques and modeling for 6G wireless communication applications: A survey, open challenges and future research directions," *IEEE Commun. Surveys Tuts.*, vol. 24, no. 4, pp. 1957–1996, 4th Quart., 2022, doi: 10.1109/COMST.2022.3205505.

[4] H. Tataria, M. Shafi, A. F. Molisch, M. Dohler, H. Sjöland and F. Tufvesson, "6G wireless systems: Vision, requirements, challenges, insights, and opportunities," *Proc. IEEE*, vol. 109, no. 7, pp. 1166–1199, Jul. 2021, doi: 10.1109/JPROC.2021.3061701.

[5] T. S. Rappaport et al., "Wireless communications and applications above 100 GHz: Opportunities and challenges for 6G and beyond," *IEEE Access*, vol. 7, pp. 78729–78757, 2019, doi: 10.1109/ACCESS.2019.2921522.

[6] D. Gesbert, M. Kountouris, R. W. Heath, C. Chae, and T. Salzer, "Shifting the MIMO paradigm," *IEEE Signal Process. Mag.*, vol. 24, no. 5, pp. 36–46, Sep. 2007.

[7] M. Giordani, M. Polese, A. Roy, D. Castor, and M. Zorzi, "A tutorial on beam management for 3GPP NR at mmWave frequencies," *IEEE Commun. Surveys Tuts.*, vol. 21, no. 1, pp. 173–196, 1st Quart., 2019.

[8] X. Zhang, G. Qiu, J. Zhang, L. Tian, P. Tang, and T. Jiang, "Analysis of millimeter-wave channel characteristics based on channel measurements in indoor environments at 39 GHz," in *Proc. 11th Int. Conf. Wireless Commun. Signal Process. (WCSP)*, Oct. 2019, pp. 1–6.

[9] D. Chizhik, J. Du, R. Feick, M. Rodriguez, G. Castro, and R. A. Valenzuela, "Path loss and directional gain measurements at 28 GHz for non-line-of-sight coverage of indoors with corridors," *IEEE Trans. Antennas Propag.*, vol. 68, no. 6, pp. 4820–4830, Jun. 2020, doi: 10.1109/TAP.2020.2972609.

[10] Y. Xing and T. S. Rappaport, "Millimeter wave and terahertz urban microcell propagation measurements and models," *IEEE Commun. Lett.*, vol. 25, no. 12, pp. 3755–3759, Dec. 2021.

[11] H. Miao et al., "Sub-6 GHz to mmWave for 5G-advanced and beyond: Channel measurements, characteristics and impact on system performance," *IEEE J. Sel. Areas Commun.*, vol. 41, no. 6, pp. 1945–1960, Jun. 2023, doi: 10.1109/JSAC.2023.3274175.H.

[12] H. Ding et al., "Ray-tracing based channel clustering and analysis at 28 GHz in conference environment," in *Proc. 14th Eur. Conf. Antennas Propag. (EuCAP)*, 2020, pp. 1–5, doi: 10.23919/EuCAP48036.2020.9135078.

[13] H. Mi et al., "Multi-scenario millimeter wave wireless channel measurements and sparsity analysis," *China Commun.*, vol. 19, no. 11, pp. 16–31, Nov. 2022, doi: 10.23919/JCC.2022.11.002.

[14] A. Mudonhi, R. D'Errico, and C. Oestges, "Analysis of multipath components distributions over a large array in indoor mmwave channels," *IEEE Trans. Antennas Propag.*, vol. 70, no. 9, pp. 8330–8336, Sep. 2022, doi: 10.1109/TAP.2022.3177439.

[15] F. Fuschini, M. Zoli, E. M. Vitucci, M. Barbiroli, and V. Degli-Esposti, "A study on millimeter-wave multiuser directional beam-forming based on measurements and ray tracing simulations," *IEEE Trans. Antennas Propag.*, vol. 67, no. 4, pp. 2633–2644, Apr. 2019, doi: 10.1109/TAP.2019.2894271.

[16] N. D. Cicco et al., "Machine learning-based line-of-sight prediction in urban manhattan-like environments," in *Proc. 17th Eur. Conf. Antennas Propag. (EuCAP)*, Florence, Italy, 2023, pp. 1–5, doi: 10.23919/EuCAP57121.2023.10133145.

[17] (SAF Tehnika, Riga, Latvia.) *SAF Tehnika—Microwave Radio Experts*. 2021. [Online]. Available: https://www.saftehnika.com/en/spectrumanalyzer

[18] E. M. Vitucci et al., "Tuning ray tracing for mm-Wave coverage prediction in outdoor urban scenarios," *Radio Sci.*, vol. 54, no. 11, pp. 1112–1128, Nov. 2019, doi: 10.1029/2019RS006869.

[19] E. M. Vitucci et al., "Ray tracing RF field prediction: An unforgiving validation," *Int. J. Antennas Propag.*, vol. 2015, pp. 1–11, Aug. 2015, doi: 10.1155/2015/184608.

[20] J. R. Abel and J. W. Wallace, "4-40 GHz permittivity measurements of indoor building materials," in *Proc. IEEE Int. Symp. Antennas Propag. USNC-URSI Radio Sci. Meeting*, 2019, pp. 105–106, doi: 10.1109/APUSNCURSINRSM.2019.8888911.

[21] D. Ferreira, I. Cuiñas, R. F. S. Caldeirinha, and T. R. Fernandes, "A review on the electromagnetic characterisation of building materials at micro- and millimetre wave frequencies," in *Proc. 8th Eur. Conf. Antennas Propag. (EuCAP)*, 2014, pp. 145–149, doi: 10.1109/EuCAP.2014.6901713.

[22] L. Possenti et al., "Improved Fabry–Pérot electromagnetic material characterization: Application and results," *Radio Sci.*, vol. 55, no. 11, pp. 1–15, Nov. 2020, doi: 10.1029/2020RS007164.

[23] "ibwave." Accessed: Jun. 3, 2023. [Online]. Available: https://ibwave.com/

[24] "Guidelines for evaluation of radio interface technologies for IMT-2020" ITU, Geneva, Switzerland, ITU Recommandation M.2412-0, 2020.

FRANCO FUSCHINI received the M.Sc. degree in telecommunication engineering and the Ph.D. degree in electronics and computer science from the University of Bologna in 1999 and 2003, respectively. He is currently an Associate Professor with the Department of Electrical, Electronic and Information Engineering "G. Marconi," University of Bologna. He is the author or coauthor of more than 30 journal papers on radio propagation and wireless system design. His main research interests are in the area of radio systems design and radio propagation channel theoretical modeling and experimental investigation. In April 1999, he got the 'Marconi Foundation Young Scientist Prize' in the context of the XXV Marconi International Fellowship Award.

LEONARDO POSSENTI received the master's degree in electronic and telecommunications engineering from the University of Florence. He is currently pursuing the Ph.D. degree in electronics, telecommunications and information technologies engineering with the University of Bologna and with a high apprenticeship program in collaboration with Teko Telekom Srl. In 2014, he attended the first semester with the Tampere University of Technology, Tampere, Finland. His activity is focused on the research topic in 5G Radio Technology, channel characterization for high frequency bands (over 6 GHz), and beamforming implementation and study on FPGA.

MARINA BARBIROLI received the Laurea degree in electronic engineering and the Ph.D. degree in computer science and electronic engineering from the University of Bologna in 1995 and 2000, respectively, where she is currently an Associate Professor with the Department of Electrical, Electronic and Information Engineering "G. Marconi." Her research interests are on propagation models for mobile communications systems, with focus on wideband channel modeling for 5G systems and beyond. Research activities includes investigation of planning strategies for mobile systems, broadcast systems and broadband wireless access systems, analysis of exposure levels generates by all wireless systems and for increasing spectrum efficiency. The research activity includes the participation to European research and cooperation programs (COST 259, COST 273 COST2100, COST IC1004, COST IRACON, and COST INTERACT) and in the European Networks of Excellence FP6-NEWCOM and FP7-NEWCOM++.

MATTIA FOSCI received the B.S. and M.Sc. degrees in telecommunications engineering from the University of Bologna, Bologna, Italy. From April 2014 to July 2015, he worked as a consultant for Vodafone IT managing, the re-routing of cellular traffic through new gen networks. He is currently the Director of the Neutral Host Design Engineering Team with JMA Wireless, Castel San Pietro Terme, Italy. He is involved in the design of 4G/5G wireless cellular coverage solutions for high-capacity venues and areas not serviced by macro networks. One of his main activities is to model 5G propagation parameters to be used in the dimensioning of the coverage system.

ENRICO M. VITUCCI (Senior Member, IEEE) is currently an Associate Professor of Applied Electromagnetics, Antennas, and Propagation with the Department of Electrical, Electronic and Information Engineering "G. Marconi," University of Bologna, where he has been a Research Associate with the Center for Industrial Research on ICT since 2011. In 2015, he was a Visiting Researcher with Polaris Wireless, Inc., Mountain View, CA, USA. He is the author or a coauthor of about 90 technical articles on international journals and conferences and a co-inventor of five international patents. He participated to several European research and cooperation programs (COST IC1004, COST IRACON, and COST INTERACT) and in the European Networks of Excellence NEWCOM and NEWCOM++. His research interests are in deterministic and wireless propagation models for 5G and beyond. He is a member of the editorial board of the *Wireless Communications and Mobile Computing*.

VITTORIO DEGLI-ESPOSTI (Senior Member, IEEE) is an Associate Professor with the "Dipartimento di Ingegneria Elettrica, Elettronica e dell'Informazione" (DEI) of the Alma Mater Studiorum, University of Bologna. From January 2015 to December 2016, he was the Director of Research with Polaris Wireless Inc., Mountain View, CA, USA. He has been an Adjunct Professor with the Helsinki University of Technology (currently Aalto University) and Tongji University, Shanghai, in 2006 and 2013, respectively. In 1998, he was a Postdoctoral Researcher with Polytechnic University, Brooklyn, NY, USA (currently NYU Polytechnic) in the group led by Professor H. L. Bertoni. He is the author or coauthor of over 140 peer-reviewed scientific papers and a co-inventor of seven international patents in the fields of applied electromagnetics, radio propagation, and wireless systems.

He is an Editor of the IEEE TRANSACTIONS ON VEHICULAR TECHNOLOGY and an Associate Editor of the *Radio Science* and IEEE ACCESS. He is the Elected Chair of the Propagation Working Group of the European Association on Antennas and Propagation and the Working Group WG1 "Radio Channels" of the EU COST Action "Interact." He has been the Vice-Chair of the European Conference on Antennas and Propagation, editions 2010 and 2011, short-Courses and Workshops Chair of the 2015 edition, and an Invited Speaker at EuCAP 2014 and ISAP 2020.